0273-2289/98/7501—0025$10.00

X-Ray Structures of Two Families of Hydrolytic Antibodies

BENOÎT GIGANT,[1] JEAN-BAPTISTE CHARBONNIER,[1] BEATRICE GOLINELLI-PIMPANEAU,[1] Z. ESHHAR,[2] BERNARD S. GREEN,[3] AND MARCEL KNOSSOW*,[1]

[1]*Laboratoire d'Enzymologie et Biochimie Structurales, Centre National de la Recherche Scientifique, Bat. 34, Avenue de la Terrasse, 91198, Gif sur Yvette Cedex, France, E-mail: knssow@lebs.cnrs-gif.fr;* [2]*Department of Immunology, The Weizmann Institute of Science, Rehovot, Israel;* [3]*Department of Pharmaceutical Chemistry, The Hebrew University School of Pharmacy, Jerusalem, Israel*

Received August 4, 1997; Accepted December 16, 1997

ABSTRACT

The catalytic mechanisms of two esterase-like catalytic antibodies (Abs) have been determined, based on kinetic data and on structures of the complexes with transition-state analogs and with a stable substrate analog of the reactions they catalyze. Both Abs stabilize the oxyanion intermediate close to the transition state in ester hydrolysis. The different geometries of the hydrogen bonds that participate in this stabilization account for most of the difference between the efficiencies of these two Abs.

Index Entries: Phosphonate hapten; ester hydrolysis; oxyanion hole; catalytic antibody; catalysis.

INTRODUCTION

The proposal that antibodies (Abs) having catalytic activity can be generated to a transition-state analog (TSA) of the reaction to be catalyzed *(1)* has proven to be widely applicable *(2,3)*. Much has been learned over the past several years about inducing Abs that promote ester hydrolysis: More than 50 antiphosphonate Abs with esterolytic activity have been reported to date, and extensive steady-state and presteady-state kinetic

*Author to whom all correspondence and reprint requests should be addressed.

studies have been performed on some of these Abs (e.g., ref. 4). Several structures of catalytic Abs with esterase-like activity complexed with their respective TSAs have also been determined *(5–8)*, so that comparisons of the catalytic mechanisms are now possible. The field of catalytic Abs with esterase-like activity has been reviewed recently *(9)*. This article presents a comparison of the structures of two families of catalytic Abs that the authors have studied.

Ab CNJ206 catalyzes the hydrolysis of *p*-nitrophenyl ester **1** with significant rate enhancement ($k_{cat}/k_{uncat} = 1600$) *(10)*. CNJ206 has been obtained by immunization with a keyhole limpet hemocyanin conjugate of phosphonate hapten **2**, and has been selected for its high affinity for the short TSA **3** *(11)*; (Fig. 1). Procedures such as this, in which the elicited hybridomas are screened for binding to a TSA, and in which only the tightest-binding clones are tested for catalysis, have led to most of the catalytic Abs known to date. In each case, there is the concern that some clones with more efficient catalytic properties might have been missed in the screening for affinity to the TSA. To improve the selection procedure, a direct assay (catELISA *[12]*) was developed that enabled screening the entire repertoire of hybridomas for catalytic activity. Ab D2.3 was elicited by immunizing BALB/c mice with a protein conjugate of the phosphonate hapten **5** and was identified by this assay. D2.3 catalyzes the hydrolysis of the nonactivated *p*-nitrobenzyl ester **4** (Fig. 1), and is the most efficient of the family of Abs obtained; it accelerates the target reaction by a factor of 10^5 *(13)*. Compared here are the X-ray structures of the Fab D2.3 complexed with the transition-state analog TSA **5** and of Fab CNJ206 complexed with TSA **3**. This allows identification of residues important for catalysis in these esterase-like Abs and analysis of the features responsible for the higher efficiency of D2.3, compared to CNJ206.

OVERALL STRUCTURE OF THE COMBINING SITE

In both the CNJ206 and the D2.3 complex structures, the ligand is located in a deep pocket in the Ab combining site at the interface between the heavy (H)- and light (L)-chain variable regions. In each complex, at least ca. 90% of the accessible surface of the ligand is buried. The bottom of the pocket, where the *p*-nitrophenyl (resp. *p*-nitrobenzyl) moiety of the ligand is found, has a marked hydrophobic character: Seven of the residues that contact the aromatic part of the ligand are apolar. The tight van der Waals interactions involved account for the specificity of both Abs for *para*-relative to *ortho*-nitrosubstituted ligands *(10,13)*, because the corresponding change in the position of substitution would require a significant rearrangement of the Fab residues to be accommodated.

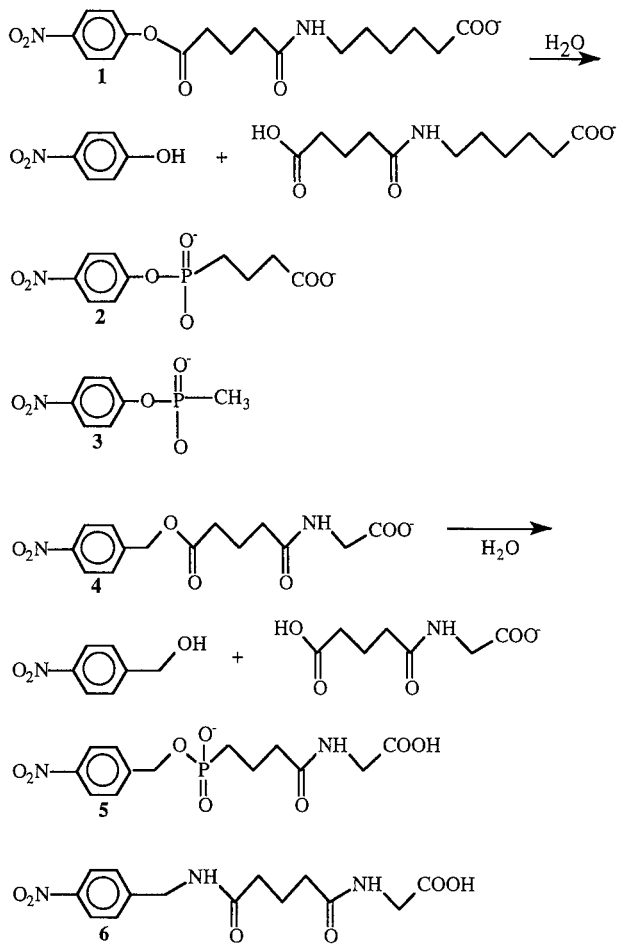

Fig. 1. Chemical reactions catalyzed by CNJ206 and D2.3 and structures of the compounds used in this study. Esters **1** and **4** are substrates hydrolyzed by CNJ206 and D2.3, respectively. *p*-nitrophenylphosphonate **2** is the TSA hapten used to elicit CNJ206. *p*-nitrobenzylamide **6** is a stable analog of the D2.3 substrate ester **4.** Crystal structures examined are those of complexes of CNJ206 with *p*-nitrophenylphosphonate **3** and of D2.3 with *p*-nitrobenzylphosphonate **5** and *p*-nitrobenzylamide **6.**

Consistent with the linkage of haptens **2** and **5** to the carrier protein through their carboxylate group *(11,12)*, the carboxylates of ligand **5** and the phosphonate of ligand **3** point toward the outside of the combining site. The overall orientation of the ligands relative to the two Abs are similar, and similar to those observed in complexes of other esterolytic Abs whose crystallographic structures have been determined *(5,7)*. This confirms the suggestion made previously that this mode of binding is favored when the hapten comprises proximal aromatic and phosphonate moieties *(6)*, although slight variations in the orientation of the aromatic groups have been noted *(9)*.

INTERACTIONS OF TSA PHOSPHONATE WITH FAB

In CNJ206, the phosphonate part of **3** makes contacts with the H3 complementarity determining region (CDR) at the entrance of the combining-site pocket. Three hydrogen bond donors that have the potential to stabilize the phosphonate can be identified, based on distance criteria; these are the NH groups of the consecutive residues Asp H96 and Tyr H97 of the H3 CDR and the $N_{\epsilon 2}$ of His H35, in the H1 CDR. The definition in the structure of two of these hydrogen bond donors (the NHs of AspH96 and TyrH97) is straightforward, but the case of His H35 is more involved. In structures of murine Fabs, the H35 residue most often establishes a hydrogen bond with Trp H47 $N_{\epsilon 1}H$ *(14)*. The two rotamers of histidine residues, which differ by a 180 degree rotation of the histidine ring, cannot be distinguished in electron-density maps, but the requirement to bring a hydrogen bond acceptor of His H35 close to the indole NH of Trp H47 ($N_{\epsilon 1}H$) defines the rotamer that is adopted by His H35 in CNJ206 as the one that brings the $N_{\delta 1}$ nitrogen close to Trp H47. The establishment of a hydrogen bond between His H35 and Trp H47 also requires the His $N_{\delta 1}$ nitrogen to be unprotonated. At pH 8.0, where the crystals were obtained and where catalysis was measured, one of the Histidine nitrogens is protonated. Because the $N_{\delta 1}$ of His H35 is unprotonated, the other nitrogen ($N_{\epsilon 2}$) of this residue is protonated, and this indeed enables His H35 to stabilize the negatively charged phosphonate of **3** (Fig. 2A). Although the identification of the three hydrogen bond donors that are in a position to stabilize the phosphonate of **3** in the CNJ206 combining site is unambiguous, it should be borne in mind that, because of the limited resolution of diffraction data on the CNJ206·**3** complex (3.2 Å), the orientation of the phosphonate around the P—O bond that links it to the *p*-nitrophenol moiety of **3** is not defined by the electron density. Therefore, additional information is required to completely define the hydrogen bonds that are actually established in the combining site of CNJ206, and, as a consequence, those that contribute to differential stabilization of the substrate and transition state, and give rise to the observed catalysis.

In the D2.3·**5** complex, both because of the better resolution of the diffraction data (1.9 Å) and because of the dissymmetry of the substituents of the phosphorous atom (Fig. 1), identification of the groups that stabilize the phosphonate of **5** is much more straightforward than in the case of the CNJ206 complex that has been studied. Three hydrogen bonds are established between D2.3 and the phosphonate of **5**. One phosphonyl oxygen (O) is within the distance and angle for hydrogen bonding with two Fab residues (Tyr H100d and Asn L34); the other P—O is similarly oriented with respect to Trp H95 and a water molecule that is not within hydrogen bonding distance with Fab residues (Fig. 2B).

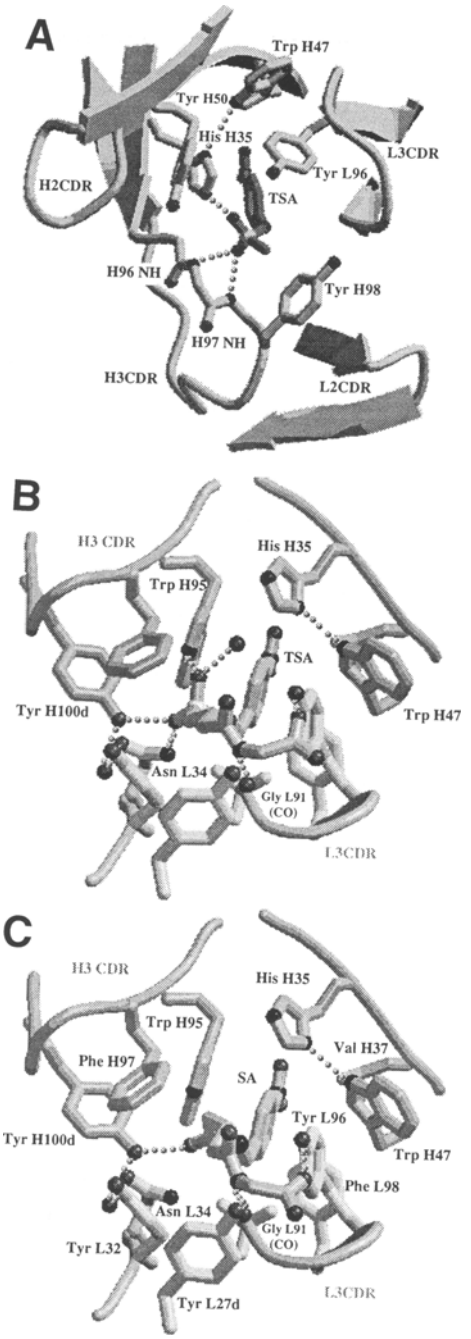

Fig. 2. Schematic views of CNJ206 and D2.3 combining-sites residues that interact with the ligands examined. Residue numbering is according to Kabat *(21)*. In panels A, B, and C, hydrogen bonds are shown as dotted lines. **(A)** Complex of CNJ206 with TSA **3**. **(B)** Complex of D2.3 with TSA **5**. **(C)** Complex of D2.3 with amide **6**, a stable analog of substrate **4**. Fig. 2A–C were drawn with Molscript *(22)*.

CATALYTIC MECHANISM

In the combining site of D2.3, residues that establish hydrogen bonds with the phosphonyl Os of **5** are likely candidates for stabilizing the oxyanion intermediate close to the transition state in the hydrolysis of 4. Because in the D2.3·**5** structure, the two phosphonyl O establish hydrogen bonds with Fab residues, there is an ambiguity left as to which is closest to the negatively charged O of the oxyanion intermediate. In order to remove this ambiguity, the structure of the complex of D2.3 with the amide **6** was determined *(15)*. Compound **6** is much more stable than the substrate **4**, whose hydrolysis is catalyzed by D2.3, because of the replacement of an ester bond by an amide bond, but otherwise it has the same geometry as the ester **4**; therefore, **6** can be considered as a substrate analog (SA). Although the negatively charged phosphonate Os in **5** establish three hydrogen bonds with the Ab (Fig. 2B), the corresponding neutral amide in **6** makes only one such interaction with Tyr H100d (Fig. 2C). The pro-S phosphonyl O in **5** is closest to the carbonyl oxygen in **6** (distance of these two O after superposition of the two complex structures: 1 Å); this identifies it as the O mimicking the oxyanion, and strongly suggests that two hydrogen bond donors, the OH of Tyr H100d and the $N_{\delta 2}H_2$ group of Asn L34, constitute the oxyanion hole in the catalysis of the hydrolysis of **4** by D2.3. The preferential stabilization of the TSA, compared to SA (three hydrogen bonds involving charged atoms vs one hydrogen bond established by neutral atoms), is consistent with the ratio of the binding constants of substrate and TSA ($1.1\ 10^5$, measured at pH 6.0 *[13]*). In the combining site, all other functional residues that can promote nucleophilic or general-base catalysis are further than 5 Å from the reaction center, which suggests that these mechanisms do not contribute significantly to catalysis by D2.3, and that oxyanion stabilization plays the major role in rate acceleration by this Ab.

In the case of Ab CNJ206, residues that are in a position to stabilize the oxyanion intermediate in the hydrolysis of **1** have been identified from the structure of the CNJ206·**3** complex. Other residues that could play a role in nucleophilic attack of the ester substrate are further than 4.1Å from the phosphorous atom of **3**, which makes such a mechanism unlikely. Because in CNJ206, His H35 is close to the phosphonate (distance P-$N_{\epsilon 2}$: 3.9 Å), there is the additional possibility that this residue would provide general-base catalysis and activate a water molecule for nucleophilic attack in the hydrolysis of **1**. To investigate this further, the variation of the catalytic activity of CNJ206, k_{cat}, as a function of pH, was studied and found to be fitted linearly between pH 5.0 and 9.5 *(16)*. The values of pKa usually reported for histidine residues (pKa = 5–8) *(17)* are within the range at which catalysis was studied. The environment of His H35 in the structures

the authors have determined does not suggest any major perturbation of its pKa during the hydrolysis reaction catalyzed by CNJ206; the simplest explanation for the dependence of catalysis on pH is therefore that histidine H35 is not involved as a general base in the rate-determining step of ester hydrolysis by CNJ206, and the most likely mechanism for catalysis of ester hydrolysis by CNJ206 is, as for D2.3, oxyanion stabilization.

EFFICIENCY OF CATALYSIS

Both the D2.3 and CNJ206 Abs catalyze ester hydrolysis by the same mechanism. The value of the catalytic acceleration of Ab D2.3 (k_{cat}/k_{uncat} = 1.1 10^5 *(13)* places this Ab among the most efficient of those with an esterase-like activity. The structures determined allow identification of a feature that accounts at least in part for this efficiency: Among the three hydrogen bonds established between the Fab and the two phosphonyl oxygens of **5**, two directed hydrogen bonds having a standard geometry (established by residues Asn L34 and Tyr H100d, which belong to the L1 and H3 CDRs) stabilize the oxyanion intermediate more efficiently than the substrate, which establishes only one such interaction (with residue Tyr H100d). Residues that should stabilize the oxyanion more efficiently than the substrate have also been identified in CNJ206; a comparison of the geometry of the corresponding hydrogen bonds to those observed in protein structures *(18)* indicates that the stabilization energy they provide to the transition state is in the lower range of those attributed to these noncovalent interactions. An additional contribution to catalysis in D2.3 could also come from the stabilization of the oxyanion through its partial protonation by Tyr H100d in the alkaline conditions of the catalysis; such a possibility is not available in CNJ206, in which the hydrogen bond donors that could stabilize the oxyanion are peptide NHs or the His H35 $N_{\epsilon 2}$, which all have much higher pKas than the tyrosine OH. All these observations are consistent with the catalytic acceleration by CNJ206 (k_{cat}/k_{uncat} = 1.6 10^3) being much smaller than that observed with D2.3.

The efficiencies of Abs CNJ206 and D2.3 are significant, and, as expected from the screening procedure used to identify this last Ab, D2.3 is much more efficient than CNJ206. Because this Ab is the most efficient of all hybridomas elicited in response to a particular phosphonate TSA, the observed value of the catalytic acceleration may also give an indication of the upper limit of the catalytic efficiencies that can be expected when such a procedure is followed for eliciting catalytic Abs. When more efficient catalysts are required, one would aim to elicit Abs that provide chemical catalysis in addition to the basic oxyanion stabilization that has been observed; this has not been found in any of the catalytic Abs structurally characterized so far. To that end, reactive immunization is a possibility that

has been shown to be successful in several cases *(19,20)*; unfortunately, because of its relatively recent implementation, none of the Abs that have been obtained through this method have had their structure determined. Such studies would define how the reactive residues recruited participate in catalysis. This in turn may provide useful indications on how to complement oxyanion stabilization through site-specific mutagenesis of Abs elicited with a phosphonate-like TSA.

REFERENCES

1. Jencks, W. P. (1969), *Catalysis in Chemistry and Enzymology*, McGraw-Hill, New York.
2. Lerner, R. A., Benkovic, S. J., and Schultz, P. G. (1991), *Science* **252,** 659–667.
3. Thomas, N. R. (1996), *Nat. Prod. Rep.* **13,** 479–511.
4. Benkovic, S. J., Adams, J. A., Borders, C. L., Janda, K. D., and Lerner, R. A. (1990), *Science* **250,** 1135–1139.
5. Zhou, G. W., Guo, J., Huang, W., Fletterick, R. J., and Scanlan, T. S. (1994), *Science* **265,** 1059–1064.
6. Charbonnier, J.-B., Carpenter, E., Gigant, B., Golinelli-Pimpaneau, B., Eshhar, Z., Green, B. S., and Knossow, M. (1995), *Proc. Natl. Acad. Sci. USA* **92,** 11,721–11,725.
7. Patten, P. A., Gray, N. S., Yang, P. L., Marks, C. B., Wedemayer, G. J., Boniface, J. J., Stevens, R. C., and Schultz, P. G. (1996), *Science* **271,** 1086–1091.
8. Charbonnier, J.-B., Golinelli-Pimpaneau, B., Gigant, B., Tawfik, D. S., Chap, R., Schindler, D. S., et al. (1997), *Science* **275,** 1140–1142.
9. MacBeath, G. and Hilvert, D. (1996), *Chem. Biol.* **3,** 433–445.
10. Zemel, R., Schindler, D. G., Tawfik, D. S., Eshhar, Z., and Green, B. S. (1994), *Mol. Immunol.* **31,** 127–137.
11. Tawfik, D. S., Zemel, R. R., Arad-Yellin, R., Green, B. S., and Eshhar, Z. (1990), *Biochemistry* **29,** 9916–9921.
12. Tawfik, D. S., Green, B. S., Chap, R., Sela, M., and Eshhar, Z. (1993), *Proc. Natl. Acad. Sci. USA* **90,** 373–377.
13. Tawfik, D. S., Lindner, A., Chap, R., Eshhar, Z., and Green, B. S. (1997), *Eur. J. Biochem.* **244,** 619–626.
14. Roberts, V. A., Stewart, J., Benkovic, S. J., and Getzoff, E. D. (1994), *J. Mol. Biol.* **235,** 1098–1116.
15. Gigant, B., Charbonnier, J.-B., Eshhar, Z., Green, B. S., and Knossow, M. (1997), *Proc. Natl. Acad. Sci. USA* **94,** 7857–7861.
16. Charbonnier, J.-B., Golinelli-Pimpaneau, B., Gigant, B., Green, B. S., and Knossow, M. (1996), *Israel J. Chem.* **36,** 143–150.
17. Fersht, A. R. (1985), *Enzyme Structure and Mechanism*, W. H. Freeman, New York.
18. Baker, E. N. and Hubbard, R. E. (1984), *Prog. Biophys. Mol. Biol.* **44,** 97–179.
19. Wagner, J., Lerner, R. A., and Barbas III, C. F. (1995), *Science* **270,** 1797–1800.
20. Wirsching, P., Ashley, J. A., Lo, C.-H. L., Janda, K. D., and Lerner, R. A. (1995), *Science* **270,** 1775–1782.
21. Kabat, E. (1991), *Sequences of Proteins of Immunological Interest*, National Institute of Health, Washington, D.C.
22. Kraulis, P. (1991), *J. Appl. Crystallogr.* **24,** 924–950.